Applied Radiation and Isotopes 191 (2023) 110518

Contents lists available at ScienceDirect

Applied Radiation and Isotopes

journal homepage: www.elsevier.com/locate/apradiso

Alternative routes for ^{64}Cu production using an 18 MeV medical cyclotron in view of theranostic applications

Gaia Dellepiane [a,*], Pierluigi Casolaro [a], Isidre Mateu [a], Paola Scampoli [a,b], Saverio Braccini [a]

[a] Albert Einstein Center for Fundamental Physics (AEC), Laboratory for High Energy Physics (LHEP), University of Bern, Sidlerstrasse 5, CH-3012 Bern, Switzerland

[b] Department of Physics "Ettore Pancini", University of Napoli Federico II, Complesso Universitario di Monte S. Angelo, 80126 Napoli, Italy

ARTICLE INFO

Keywords:
Copper-64
Theranostics
Cross sections
Proton irradiation
Medical cyclotron
Solid targets
PET imaging
Target radiotherapy

ABSTRACT

Radiometals play a fundamental role in the development of personalized nuclear medicine. In particular, copper radioisotopes are attracting increasing interest since they offer a varying range of decay modes and half-lives and can be used for imaging (^{60}Cu, ^{61}Cu, ^{62}Cu and ^{64}Cu) and targeted radionuclide therapy (^{64}Cu and ^{67}Cu), providing two of the most promising true theranostic pairs, namely ^{61}Cu/^{67}Cu and ^{64}Cu/^{67}Cu. Currently, the most widely used in clinical applications is ^{64}Cu, which has a unique decay scheme featuring β^+-, β^--decay and electron capture. These characteristics allow its exploitation in both diagnostic and therapeutic fields. However, although ^{64}Cu has extensively been investigated in academic research and preclinical settings, it is still scarcely used in routine clinical practice due to its insufficient availability at an affordable price. In fact, the most commonly used production method involves proton irradiation of enriched ^{64}Ni, which has a very low isotopic abundance and is therefore extremely expensive. In this paper, we report on the study of two alternative production routes, namely the ^{65}Cu(p,pn)^{64}Cu and ^{67}Zn(p, α)^{64}Cu reactions, which enable low and high ^{64}Cu specific activities, respectively. To optimize the ^{64}Cu production, while minimizing the mass of copper used as a target in the first case, or the co-production of other copper radioisotopes in the second case, an accurate knowledge of the production cross sections is of paramount importance. For this reason, the involved nuclear reaction cross sections were measured at the Bern medical cyclotron laboratory by irradiating enriched ^{65}CuO and enriched ^{67}ZnO targets. On the basis of the obtained results, the production yield and purity were calculated to assess the optimal irradiation conditions. Several production tests were performed to confirm these findings.

1. Introduction

^{64}Cu ($t_{1/2}$ = 12.7006 h, EC: 44.0%, β^-: 38.5%, β^+: 17.5%) (IAEA, 2022) is an attractive radioisotope for clinical applications in nuclear medicine for both diagnostic and therapeutic purposes. This is due to its unique decay scheme featuring three different decay modes, namely electron capture, β^- and β^+ decay. Its short positron range ($E_{\beta^+}^{max}$=652.62(21) keV), similar to the one of ^{18}F, allows for high-resolution PET imaging, enhanced by the absence of an abundant γ-ray emission. On the other hand, the Auger electrons resulting from electron capture and the β^- particles can be used for targeted radionuclide therapy (Blower et al., 1996). ^{64}Cu radiopharmaceuticals can thus be used for quantitative PET imaging to assess the radiation dose prior performing targeted radiotherapy with ^{64}Cu (Jauregui-Osoro et al., 2021) (earning ^{64}Cu the name of theranostic agent (Gutfilen et al., 2018)) or its therapeutic partner ^{67}Cu ($t_{1/2}$ = 61.83 h, β^-: 100%).

Due to the increasing interest for this radionuclide in nuclear medicine, several ^{64}Cu production methods have been proposed. The most widely used is based on the reaction ^{64}Ni(p,n)^{64}Cu (Szelecsényi et al., 1993; McCarthy et al., 1997), which allows obtaining high production yields of no-carrier-added ^{64}Cu with low energy protons, easily reachable with small medical cyclotrons. Although these accelerators are available in many nuclear medicine departments, the high cost of isotopically enriched ^{64}Ni (natural abundance 0.926%) makes this route prohibitively expensive for clinical applications. For this reason, alternative production methods have been explored, including deuteron irradiation of natural zinc (Bonardi et al., 2003; Hilgers et al., 2003; Abbas et al., 2006) and the use of nuclear reactors via the ^{63}Cu(n,γ)^{64}Cu (Bokhari et al., 2010; Chakravarty et al., 2020) and ^{64}Zn(n,p)^{64}Cu (Zinn et al., 1994) reactions, which, however, provide low specific activities. The ^{64}Zn(n,p)^{64}Cu reaction, together with the ^{65}Cu(n,2n)^{64}Cu reaction, was also investigated by using fast neutron generators (Kin et al., 2013; Kawabata et al., 2015; Capogni et al., 2020;

* Corresponding author.
E-mail address: gaia.dellepiane@lhep.unibe.ch (G. Dellepiane).

https://doi.org/10.1016/j.apradiso.2022.110518
Received 27 August 2022; Received in revised form 13 October 2022; Accepted 14 October 2022
Available online 20 October 2022

Dellepiane, 2022), although such machines are scarcely available. In addition, proton-induced reactions of enriched ^{66}Zn (Szelecsényi et al., 2005), ^{67}Zn (Szelecsényi et al., 2014) and ^{68}Zn (Hilgers et al., 2003; Szelecsényi et al., 2005) targets were studied. Among these, the ^{67}Zn(p, α)^{64}Cu reaction reaches its maximum cross section at about 14 MeV, making small medical cyclotrons suitable for ^{64}Cu production.

In the framework of a research program focused on novel radionuclides for theranostics at the Bern medical cyclotron laboratory (Braccini et al., 2019), the production of ^{64}Cu with low and high specific activity was investigated via proton irradiation of enriched ^{65}CuO and enriched ^{67}ZnO solid targets.

In the case of the reaction ^{65}Cu(p,pn)^{64}Cu, no other copper radioisotopes are produced during the irradiation but only very low specific activities can be obtained since stable Cu is used as the target material. This leads to interferences in radiolabelling, as the non-radioactive carrier copper competes with ^{64}Cu in binding to the chelator. However, it is possible to use the produced ^{64}Cu in the form of [^{64}Cu]$CuCl_2$ as a radiopharmaceutical for PET imaging (Chakravarty et al., 2016), if the clinically relevant amount does not manifest any toxicity concerns due to "cold" Cu (Chakravarty et al., 2020).

For the ^{67}Zn(p, α)^{64}Cu reaction, the main impurities to be kept under control in the energy range of PET medical cyclotrons are ^{61}Cu, obtained from ^{64}Zn via the ^{64}Zn(p, α)^{61}Cu reaction, and ^{67}Cu, obtained from ^{70}Zn via the ^{70}Zn(p, α)^{67}Cu reaction. It is important to underline that both ^{64}Zn and ^{70}Zn are present as impurities in the target material, even if a highly-enriched ^{67}Zn pellet is used. The quantity of ^{61}Cu can prolong the waiting time before medical applications, while the presence of ^{67}Cu may limit the application period of the labeled compounds. To maximize ^{64}Cu activities while minimizing ^{61}Cu and ^{67}Cu impurities, the precise knowledge of the reaction cross sections as a function of the beam energy is fundamental.

In this paper we report on the cross-section measurement of the nuclear reactions ^{65}Cu(p,pn)^{64}Cu, ^{67}Zn(p, α)^{64}Cu and ^{64}Zn(p, α)^{61}Cu, performed at the Bern medical cyclotron laboratory to optimize the production of ^{64}Cu, by maximizing the radionuclidic purity and the production yield. Several production tests were performed using enriched ^{65}CuO and enriched ^{67}ZnO solid targets to confirm our predictions based on cross-section measurements.

2. Materials and methods

The Bern medical cyclotron laboratory is located at the Bern University Hospital (Inselspital) (Braccini, 2013). It hosts an IBA Cyclone 18/18 HC, accelerating H^- ions to a nominal energy of 18 MeV with a current range from a few pA to 150 μA (Auger et al., 2015). The facility is characterized by two bunkers with independent access, allowing commercial GMP ^{18}F production to take place during the night and multidisciplinary research activities during the day (Braccini and Scampoli, 2016). The cyclotron features six ^{18}O-enriched water targets, an IBA Nirta Solid Target Station (STS) and a 6-m-long Beam Transfer Line (BTL) that brings the beam to the second bunker. The BTL is equipped with beam focusing and diagnostic systems, including a non-destructive two-dimensional beam profiler based on scintillating doped silica fibers passing through the beam. The detector, named UniBEaM, was developed by our group and commercialized by the company D-Pace (Auger et al., 2016; Potkins et al., 2017). The BTL is characterized by an extracted beam energy of (18.3 ± 0.3) MeV (Nesteruk et al., 2018; Häffner et al., 2019) and was used for the cross-section measurements presented in this paper.

The ^{64}Cu production tests were performed using the STS, customized with automatic target loading and delivery systems to minimize the dose to personnel (Dellepiane et al., 2022b). In particular, the irradiated target can be sent either to one hot-cell in the nearby GMP radio-pharmacy or to a receiving station located in the BTL bunker. The latter option is used when the target needs to be transported to external laboratories for chemical processing or transferred to the physics laboratory of the facility for gamma spectrometry. For this purpose, a N-type high-purity germanium (HPGe) detector (Canberra 2019) was used. The detector is coupled to a preamplifier and to a Lynx® digital signal analyzer. The spectrum of the source is acquired with the Genie2K software (Mirion Technologies, 2022) in the case of a single measurement and with the Excel2Genie (Forgács et al., 2014) Microsoft Excel application for repeated measurements. The analysis is carried out with the InterSpec software (Sandia National Laboratories, 2022), developed by the Sandia National Laboratories. The efficiency calibration was performed in accordance with the international standard (International Standard, 2021) by means of a multi-peak γ source. The calibration source was measured at distances up to 10 cm from the detector, thanks to a custom-designed plexiglass ladder with equally spaced levels 1 cm apart. At each level, the measured efficiencies as a function of the gamma energies are fitted using a parametric least-squares fit. The average uncertainty of the efficiencies is about 3%.

Table 1
Isotopic abundance of the enriched ^{65}CuO powder by Isoflex used in this study.

	^{63}Cu	^{65}Cu
^{65}Cu-enr. [%]	0.33	99.67

Table 2
Isotopic abundance of the enriched ^{67}ZnO powder by Isoflex used in this study.

	^{64}Zn	^{66}Zn	^{67}Zn	^{68}Zn	^{70}Zn
^{67}Zn-enr. [%]	1.56	3.88	89.60	4.91	0.05

Table 3
Physical properties of copper radionuclides (IAEA, 2022). The values in parentheses are the uncertainties referred to the last digits of the value. BR is the branching ratio.

Radionuclide	$t_{1/2}$	Decay mode: [%]	E_γ [keV]	BR_γ [%]
^{61}Cu	3.339(8) h	ec + β^+: 100	282.956(10)	12.7(20)
^{62}Cu	9.67(3) min	ec + β^+: 100	1172.97(10)	0.342(17)
^{64}Cu	12.7006(20) h	ec + β^+: 61.5 β^-: 38.5	1345.77(6) –	0.472(4) –
^{67}Cu	61.83(12) h	β^-: 100	184.577(10)	48.7(3)

The production of ^{64}Cu was studied by irradiating both enriched ^{65}CuO and enriched ^{67}ZnO powders, purchased from Isoflex (http://www.isoflex.com/), whose isotopic compositions are reported in Table 1 and Table 2, respectively. In the latter case, ^{61}Cu and ^{67}Cu are also produced during the irradiation via the secondary reactions ^{64}Zn(p, α)^{61}Cu and ^{70}Zn(p, α)^{67}Cu, respectively; as for enriched ^{65}CuO, no other copper radioisotopes were observed.

The decay properties of the radionuclides of interest are listed in Table 3.

2.1. Cross-section measurements

The experimental procedure used in this work was the same as our previous studies on cross-section measurements (Carzaniga and Braccini, 2019; Dellepiane et al., 2022a; Braccini et al., 2022) and is described in detail in Carzaniga et al. (2017). This method is based on the irradiation of the full mass of a thin target by a proton beam with a constant surface distribution and has the advantage that the target has not to be necessarily uniform in thickness, provided that the energy of the protons can be considered constant within its mass.

The beam was flattened by the optical elements of the BTL and monitored online with the UniBEaM detector. The beam current hitting the target material was measured by means of a custom target station connected to an electrometer (B2985 A Keysight). The station provides a beam of controlled diameter thanks to an 8 mm collimator. To perform irradiations below 18 MeV, the beam energy was degraded by means of aluminum attenuator discs placed in front of the target and

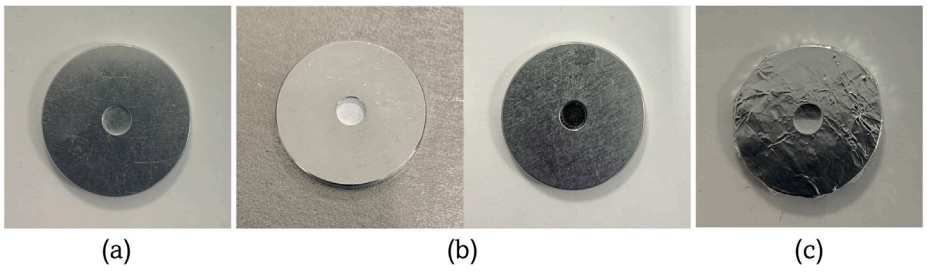

Fig. 1. Preparation procedure for the targets used for the cross-section measurements: (a) empty aluminum disc; (b) aluminum disc filled with enriched ^{67}ZnO (left) and enriched ^{65}CuO (right) powder; (c) aluminum disc covered with a 13-μm-thick aluminum foil.

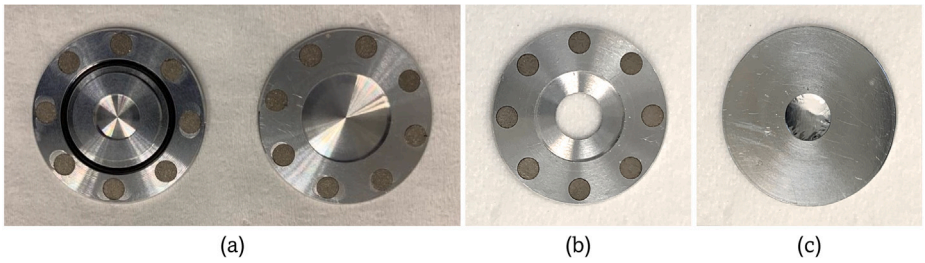

Fig. 2. (a) The cup (left) and the lid (right) of the coin target; (b) lid with a 7-mm-diameter hole; (c) 13-μm-thick aluminum foil inserted inside the coin to prevent the pellet leakage during the irradiation.

was determined using the SRIM-2013 Monte Carlo code (Ziegler and Manoyan, 2013).

For both target materials, about 1.4 mg of powder were suspended in distilled water and deposited in the 4.2-mm-diameter, 0.8-mm-deep pocket of an aluminum disc (Fig. 1a: diameter 22.8 mm, thickness 2 mm), as shown in Fig. 1b. Once the water had completely evaporated by means of a heating plate, the deposited mass was measured with an analytical balance (Mettler Toledo AX26 DeltaRange) with a sensitivity of 2 μg and a reproducibility of 4 μg. To guarantee that the material is kept within the pocket throughout the irradiation and measurement procedure, the targets were then sealed with a 13-μm-thick aluminum foil (Fig. 1c). With this procedure, target thicknesses up to 14 μm were achieved, allowing to consider the beam energy constant within the uncertainties over the full irradiated mass.

Both materials were irradiated at different energies with currents of about 8.5 nA for an average of 12 min in the case of CuO and of 23 min in the case of ZnO. After each irradiation, the produced activity was measured by gamma spectrometry with the HPGe detector. In all measurements, the count frequency was sufficiently low to limit negative effects due to pile up and random summing (dead time below 2%).

3. Study of production yield and purity

Aiming at an optimized production of ^{64}Cu, a study of the Thick Target Yield (TTY) and of the purity was performed on the basis of the results obtained. From the cross-section measurements, the TTY as a function of the proton energy on target (entry energy) E can be calculated using the following formula

$$TTY(E) = \frac{A(t_i)}{I \cdot t_i} = \frac{(1 - e^{-\lambda \cdot t_i})}{m_{mol} \cdot q} \int_{E_{th}}^{E} \frac{\sigma(E')}{S_p(E')} dE' \quad (1)$$

where t_i is the irradiation time, I the current on target, $A(t_i)$ the activity produced at the End of Beam (EoB), λ the decay constant, $\sigma(E')$ the cross section as a function of the proton kinetic energy E', $S_p(E')$ is the mass stopping power for the target material, E_{th} is the threshold energy for the considered reaction, N_A the Avogadro constant, m_{mol} the average molar mass of the target material, η the number of target atoms of the desired species per molecule and q the charge of the projectile. The mass stopping power was calculated using SRIM.

Given a sample containing a mixture of N radioisotopes, the purity of the radionuclide of interest X is given by

$$P_X = \frac{A_X}{\sum_i^N A_i} \quad (2)$$

where A_i is the activity of the ith radionuclide.

If a thin target is used, so that the protons are not stopped therein, the production yield, Y(E), can be defined as

$$Y(E) = TTY(E) - TTY(E_{out}) \quad (3)$$

where E_{out} is the proton energy after the target, calculated by using SRIM.

3.1. ^{64}Cu production tests

The targets used for production tests were prepared by compressing approximately 69 mg and 59 mg of enriched ^{65}CuO and enriched ^{67}ZnO, respectively, with the application of an axial force of about $4 \cdot 10^4$ N. The thicknesses of the obtained 6-mm-diameter disc-shaped pellets could not be measured due to their high fragility and were therefore calculated on the basis of the theoretical densities of CuO and ZnO (6.31 g/cm^3 and 5.61 g/cm^3, respectively National Center for Biotechnology Information, 2022), resulting in 0.39 mm and 0.37 mm, respectively. These values were used in all calculations and SRIM simulations.

The pellets were placed in a special capsule – called coin – consisting of two aluminum halves kept together by permanent magnets (Fig. 2a). The coin was conceived and built by our group to irradiate compressed powder pellets or solid foils and has been successfully used to produce several radionuclides (Dellepiane et al., 2021), in particular ^{44}Sc (van der Meulen et al., 2020), ^{68}Ga (Braccini et al., 2022) and ^{155}Tb (Dellepiane et al., 2022a; Favaretto et al., 2021).

The back part of the coin hosts the pellet and an O-ring to prevent the possible leakage of molten material or of any gas produced during the irradiation. To avoid overheating during the irradiation, the lid and the cup are helium-cooled and water-cooled, respectively.

The energy of the protons reaching the target material was set by adjusting the thickness of the lid, in order to optimize the production yield and the radionuclidic purity. In particular, a lid with a 7-mm-diameter hole (Fig. 2b) was used in some production tests in order not

to degrade the beam energy. In this case, a 13-μm-thick aluminum foil was placed inside the coin to prevent possible leakage of the pellet. (Fig. 2c).

The current was measured throughout each irradiation by connecting the body of the STS to the B2985 A Keysight electrometer. The effective current hitting the 6-mm-diameter pellet was assessed by measuring the 2D beam profiles with radiochromic films (Casolaro, 2021) and was known with an uncertainty of 10%.

Two production tests were carried out by irradiating the 0.39-mm-thick enriched ^{65}CuO target with the highest achievable energies. In this regard, one irradiation was carried out in the BTL by means of an adapted version of the solid target station used for cross-section measurements, so that an energy of (18.2 ± 0.4) MeV could be reached.

The activity produced was assessed with the HPGe detector; in all measurements, the distance between the target and the crystal was adjusted to minimize pile up and random summing, resulting in a dead time of less than 1%.

As for the 0.37-mm-thick enriched ^{67}ZnO pellet, two irradiations were performed with the STS at energies around 16.5 MeV. The target was then measured several times with the HPGe detector to study the purity of ^{64}Cu as a function of time. In all measurements the dead time was below 5%.

For both materials, after each irradiation the pellet was let to decay completely.

4. Experimental results

4.1. Cross-section measurements

The experimental uncertainties in cross-section measurements include the flatness of the beam (5%), the beam current integration (1%), the HPGe detector efficiency (3%) and the target mass measurements (up to 5%). Considering the ^{65}Cu(p,pn)^{64}Cu and ^{67}Zn(p, α)^{64}Cu reactions, the main contribution was given by the statistical uncertainty of the 1346-keV peak (up to 12% and 15%, respectively), due to its low branching ratio. As for the ^{64}Zn(p, α)^{61}Cu reaction, the main uncertainties were due to the 283-keV peak (up to 20%) and to its branching ratio (~16%). All the contributions were summed in quadrature to obtain the overall experimental uncertainty.

Enriched ^{65}CuO

In the energy range of interest, ^{64}Cu was the only copper radioisotope observed by irradiating the 99.67% enriched ^{65}CuO material. It is produced via the ^{65}Cu(p,pn)^{64}Cu reaction. Fig. 3 shows the measured cross section, as well as TENDL-2021 predictions (Koning and Rochman, 2012) and the data available in the literature (Levkowskij, 1991; Meadows, 1953; Cohen et al., 1954; Collé et al., 1976; Brinkman et al., 1977). For completeness, the numerical cross-section values are reported in the Appendix (Table 6).

According to TENDL, ^{62}Cu should be produced in small quantities via the ^{63}Cu(p,pn)^{62}Cu reaction at energies above 13 MeV. However, due to the low activity produced and the low intensity of γ emissions, it was not possible to detect any signal of ^{62}Cu in this experiment. In any case, the ^{62}Cu half-life is sufficiently short to neglect its production.

Enriched ^{67}ZnO

In the investigated energy region, ^{64}Cu is produced from ^{67}Zn via the (p, α) reaction. The results of the ^{67}Zn(p, α)^{64}Cu cross-section measurements are presented in Fig. 4; for completeness, the numerical values are reported in the Appendix (Table 7).

Our measurements are in good agreement with the data available in the literature (Szelecsényi et al., 2014; Levkowskij, 1991). In accordance with the findings of Takacs et al. (2002), the values presented in Levkowskij (1991) were scaled by a factor of 0.8, on the basis of

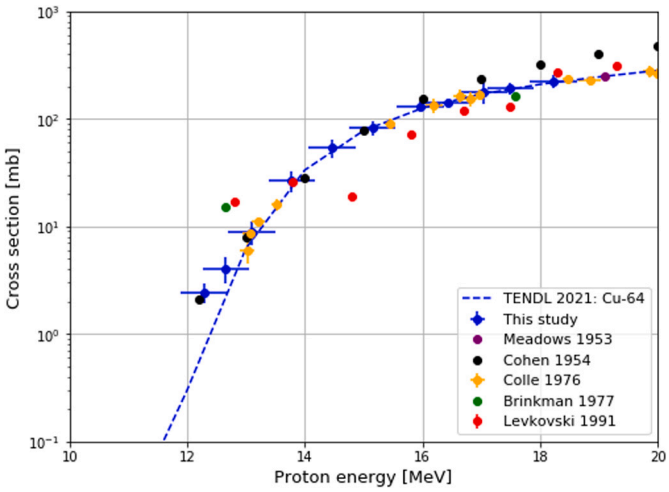

Fig. 3. ^{65}Cu(p,pn)^{64}Cu nuclear cross section.

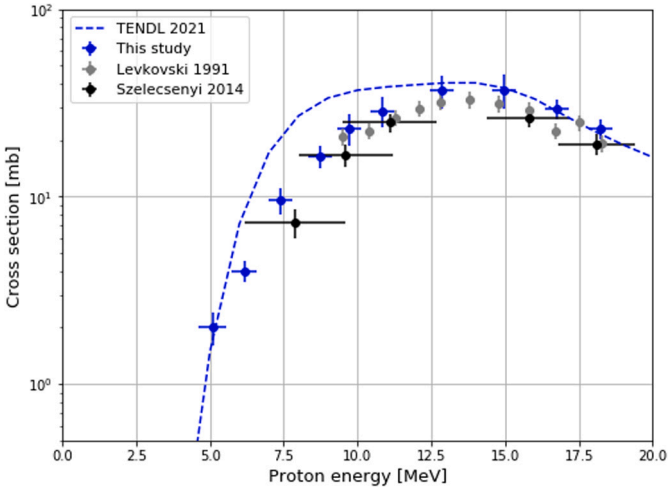

Fig. 4. ^{67}Zn(p, α)^{64}Cu nuclear cross section.

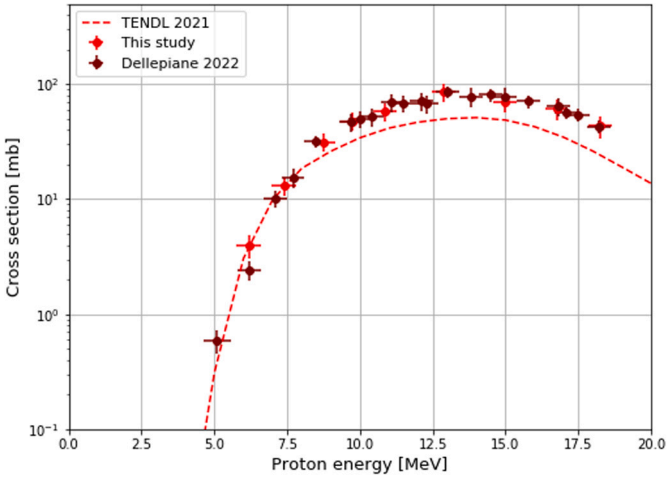

Fig. 5. ^{64}Zn(p, α)^{61}Cu nuclear cross section.

the currently accepted value of the monitor reaction that was used by Levkovskij in his original work. TENDL predictions reproduce well the experimental data for energies above 12 MeV, while at lower energies some discrepancies are observed.

^{61}Cu is the only impurity observed by irradiating a 89.60% enriched ^{67}ZnO target. In the energy range of interest, it results from ^{64}Zn via the (p, α) reaction. The ^{64}Zn(p, α)^{61}Cu nuclear cross-section measurements are presented in Fig. 5; for completeness, the numerical values are reported in the Appendix (Table 7). The results obtained in this study are in good agreement with our previous findings (Dellepiane et al., 2022d). TENDL predictions reproduce well the experimental data for energies below 8 MeV, while at higher energies some discrepancies are observed.

According to TENDL, ^{67}Cu should also be produced in the energy range of interest via the ^{70}Zn(p, α)^{67}Cu reaction. However, due to the low fraction of ^{70}Zn in the target material (Table 2), the ^{67}Cu production cross section is of the order of microbarns and could not be measured in this experiment.

4.2. Production tests

A study of the production yield (Y) and the purity (P) was performed on the basis of the obtained results in order to optimize the ^{64}Cu production.

Enriched ^{65}CuO

^{64}Cu is the only copper radioisotope produced in the irradiation of a 99.67% enriched ^{65}Cu target, as the production of the short-lived ^{62}Cu at energies above 13 MeV is negligible. The ^{64}Cu thick target yield (Eq. (1)) as a function of energy is shown in Fig. 6a and 6b for an irradiation time of 1 h and in saturation condition, respectively. In both cases, the highest ^{64}Cu TTY can be obtained with the maximum achievable energy on target.

In order to maximize the specific activity of ^{64}Cu, a study of the production yield at saturation as a function of the mass of the copper target was carried out (Fig. 7). In this study, the highest achievable energy on target was considered, which for our medical cyclotron is 17.8 MeV in the out-port of the STS, if a $\sim$ 10 μm Havar beam extraction window foil is used. In this condition, for 30 mg of ^{65}Cu, a ^{64}Cu yield of 358 MBq/μA is achievable according to our findings. Considering an average current of 10 μA on target, which can be easily reached with the STS, a ^{64}Cu specific activity of 120 MBq/mg is obtained. Clinically relevant doses of [^{64}Cu]$CuCl_2$ for PET imaging of cancer in human patients are of (200–450) MBq (Capasso et al., 2015; Avila-Rodriguez et al., 2017), which translates into an intake of 0.06 mg Cu/kg for a 60 kg patient. Since it has been reported that toxicity concerns due to cold Cu are manifested in humans when the intake of copper is >5 mg Cu/kg body weight (Aggett, 1999), our result is much below the toxic limit. Furthermore, the amount of cold Cu in clinically relevant dose of [^{64}Cu]$CuCl_2$ could be further minimized by considering higher proton energies, as the cross section of ^{64}Cu was found to increase at 18 MeV, reaching its maximum, according to TENDL-2021, at around 24 MeV.

To confirm the calculations based on cross-section measurements, two production tests were performed. The entry energies, the irradiation parameters and the activities obtained are reported in Table 4. The production yield of ^{64}Cu calculated in our irradiation conditions from Eq. (3) and the experimental results are shown in Fig. 8 as a function of the proton energy. A good agreement was found between the experimental measurements and the predictions based on our cross sections.

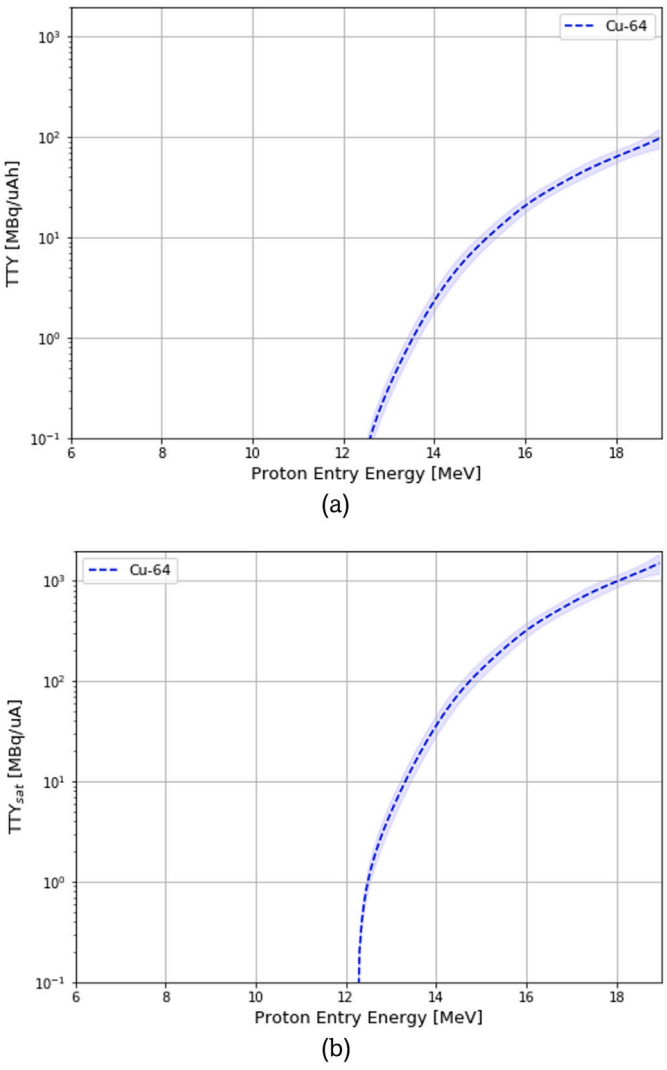

Fig. 6. ^{64}Cu thick target yield for a 99.67% enriched ^{65}Cu target, considering an irradiation time of 1 h (a) and in saturation condition (b). The bands correspond to the maximum and minimum activity calculated on the basis of the measured cross sections.

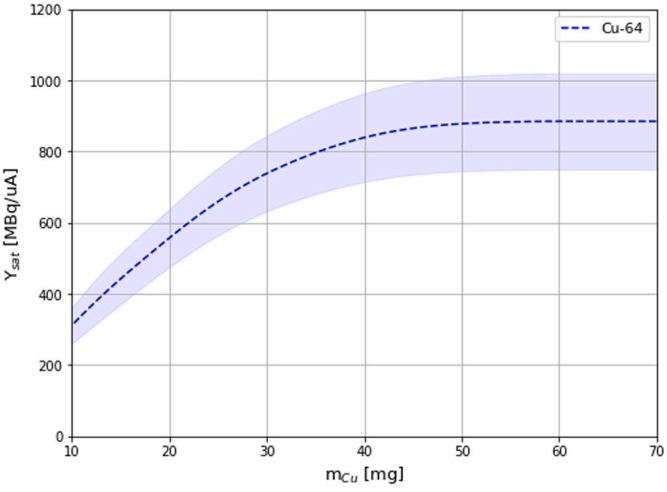

Fig. 7. ^{64}Cu saturation yield for a 6-mm-diameter 99.67% enriched ^{65}CuO target with an entry energy of 17.8 MeV, as a function of the copper mass. The bands correspond to the maximum and minimum yield calculated on the basis of the measured cross sections.

Table 4
Irradiation parameters and ^{64}Cu yield at EoB obtained irradiating a 0.39-mm-thick enriched ^{65}CuO pellet. The values in parentheses are the yield calculations based on the cross-section measurements.

E_{in}	E_{out}	Q	Y(^{64}Cu)	P(EoB)
[MeV]	[MeV]	$\times 10^{-4}$ [μAh]	[MBq/μAh]	[%]
18.2 ± 0.4	13.1 ± 0.4	12.8 ± 1.3	71 ± 7 *(70)*	100 *(100)*
17.5 ± 0.4	12.1 ± 0.4	9.6 ± 1.0	54 ± 6 *(51)*	100 *(100)*

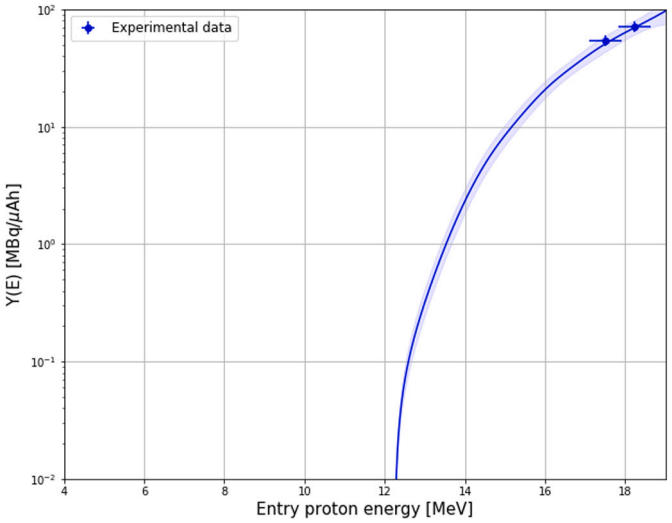

Fig. 8. ^{64}Cu production yield calculated from the measured cross sections in our irradiation conditions, compared to the experimental results of two irradiations using 0.69-mm-thick 99.67% enriched ^{65}CuO target. The bands correspond to the maximum and minimum yield calculated on the basis of the measured cross sections.

Enriched ^{67}ZnO

The thick target yields of ^{64}Cu, ^{61}Cu and ^{67}Cu are shown in Fig. 9 as a function of the entry energy. In case of ^{64}Cu and ^{61}Cu, the TTYs were calculated from the cross-section measurements reported in this paper, considering the 89.60% enriched ^{67}Zn target material (Table 2). As for ^{67}Cu, the TTY was calculated on the basis of the ^{70}Zn(p, α)^{67}Cu nuclear cross sections measured by irradiating a 98.75% enriched ^{70}ZnO target in the framework of our research program on Cu radionuclides (Dellepiane et al., 2023). In all cases the irradiation time t_i is set to 1 h. The radionuclidic purity, calculated from Eq. (2), is constant for energies above 14 MeV, while the highest production yield can be reached by irradiating the target with the maximum achievable energy, as shown in Fig. 10a.

Since the main impurity is ^{61}Cu and its half-life is much shorter than that of ^{64}Cu, the radionuclidic purity can be improved by considering long irradiation times and/or letting the target decay after the end of irradiation. In both cases, however, it must be taken into account that the amount of the long-lived ^{67}Cu present in the sample increases. In saturation condition and considering the maximum reachable energy of 17.8 MeV, a production yield of 479 MBq/μA with a purity of about 96% can be achieved (Fig. 10b). In these conditions, the presence of ^{67}Cu leads a decrease in purity of 0.005% compared to the 1 h irradiation case.

Considering the same irradiation conditions, the percentage of impurities present in the sample and the radionuclidic purity as a function of time can be calculated, as shown in Fig. 11a and 11b. In Fig. 11b the fraction of the remaining ^{64}Cu activity is also reported. From the plots, it results that after about 10 h the purity is above 99%.

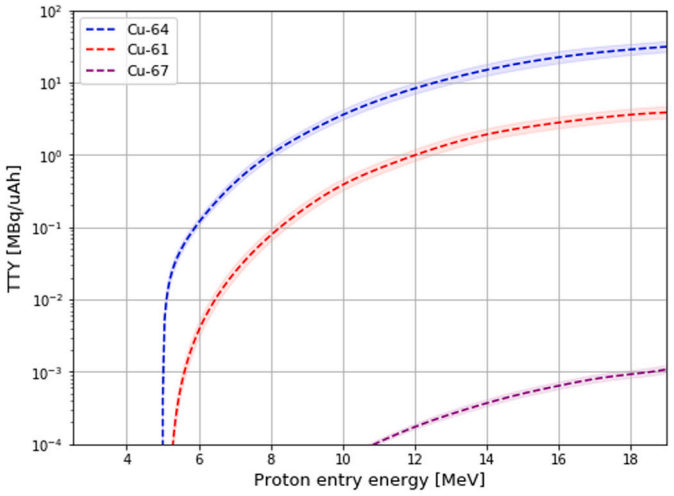

Fig. 9. ^{64}Cu, ^{61}Cu and ^{67}Cu thick target yields for a 89.60% enriched ^{67}ZnO target, considering an irradiation time of 1 h. The bands correspond to the maximum and minimum yield calculated on the basis of the measured cross sections.

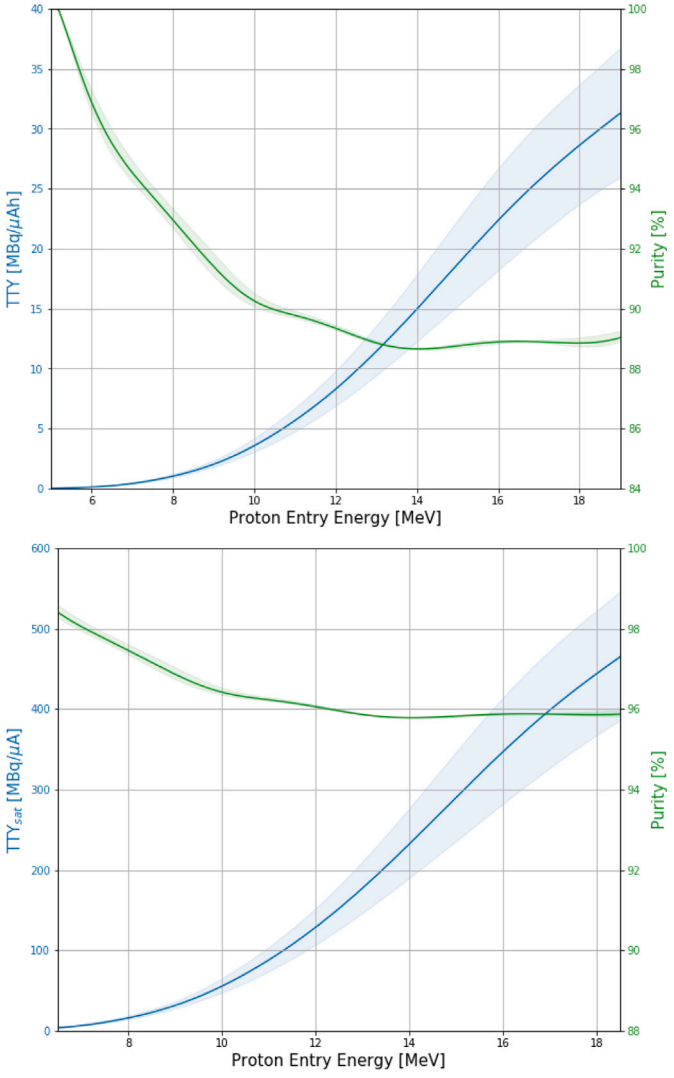

Fig. 10. ^{64}Cu thick target yield and purity for a 89.60% enriched ^{67}Zn target, considering an irradiation time of 1 h (a) and in saturation condition (b). The bands correspond to the maximum and minimum yield calculated on the basis of the measured cross sections.

Table 5
Irradiation parameters, ^{64}Cu and ^{61}Cu yields and radionuclidic purity obtained irradiating a 0.37-mm-thick enriched ^{67}ZnO pellet. The values in parentheses are the yield calculations based on the cross-section measurements.

E_{in}	E_{out}	Q	Y(^{64}Cu)	Y(^{61}Cu)	P(EoB)	P(10 h)
[MeV]	[MeV]	$\times 10^{-4}$ [μAh]	[MBq/μAh]	[MBq/μAh]	[%]	[%]
17.3 ± 0.4	12.8 ± 0.4	2.7 ± 0.3	16.1 ± 1.7 *(15.9)*	2.1 ± 0.3 *(2.0)*	88.3 ± 1.0 *(88.8)*	97.4 ± 1.0 *(97.4)*
16.4 ± 0.4	11.7 ± 0.4	1.3 ± 0.1	16.1 ± 1.8 *(16.3)*	2.1 ± 0.3 *(2.1)*	88.3 ± 1.2 *(88.6)*	97.3 ± 1.3 *(97.3)*

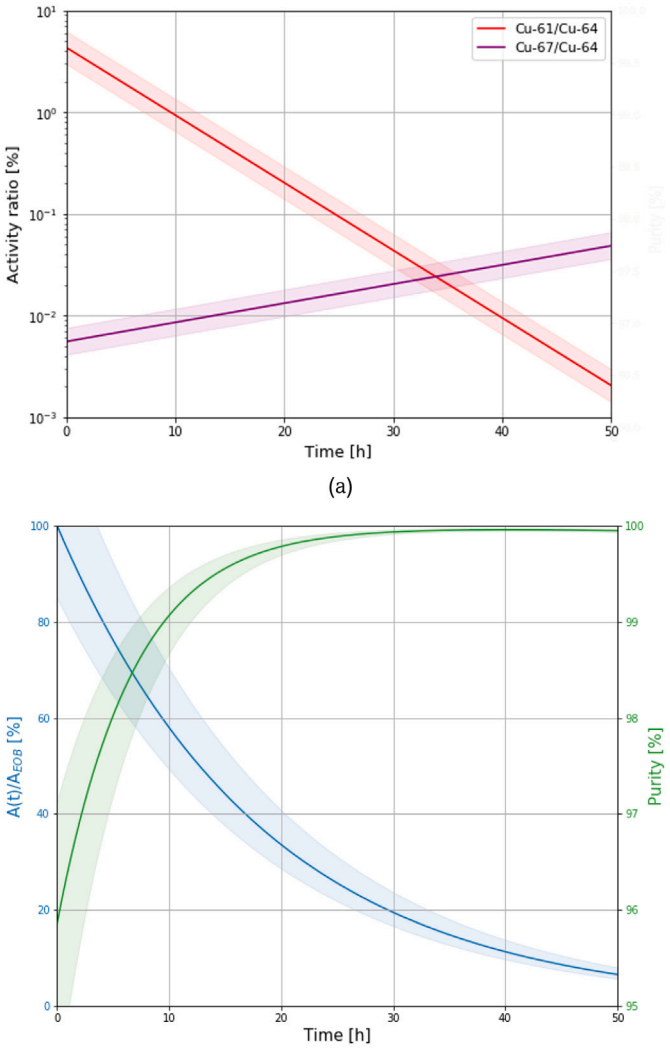

Fig. 11. (a) ^{61}Cu/^{64}Cu and ^{67}Cu/^{64}Cu activity ratio and (b) ^{64}Cu activity fraction and purity as a function of time, considering an entry energy of 17.8 MeV and saturation conditions. The bands correspond to the maximum and minimum activity calculated on the basis of the measured cross sections.

To confirm the calculations based on cross-section measurements, two production tests were performed with the STS. The production yield and the radionuclidic purity calculated in our irradiation conditions are shown in Fig. 12 as a function of the entry energy, together with the experimental measurements. The entry energies, the irradiation parameters and the activities obtained from the production tests are reported in Table 5. A good agreement was found between the experimental measurements and the predictions based on our cross sections.

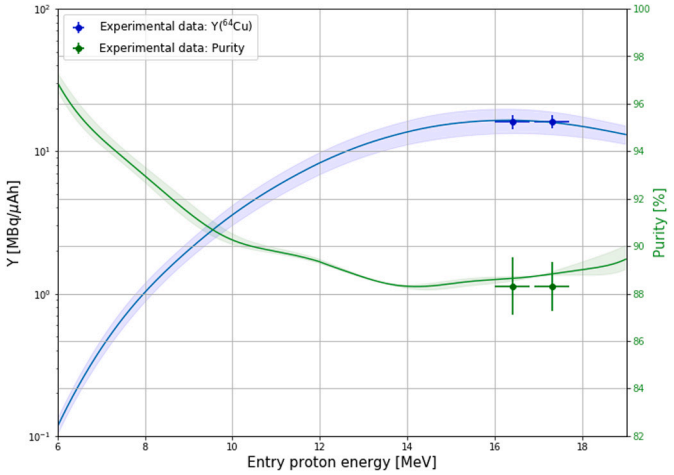

Fig. 12. ^{64}Cu production yield calculated from the measured cross sections in our irradiation conditions, compared to the experimental results for two irradiations using 0.63-mm-thick 89.60% enriched ^{67}ZnO target. The bands correspond to the maximum and minimum yield calculated on the basis of the measured cross sections.

5. Conclusions and outlook

^{64}Cu is gaining increasing interest in nuclear medicine because of its unique physical characteristics that allow it to be used for both diagnostic and therapeutic purposes. Furthermore, considering the β^+-decay mode, it forms a promising true theranostic pair with the β^- emitter ^{67}Cu.

The major deterrent to a wider use of ^{64}Cu-labeled radiotracers in nuclear medicine is the limited availability of this radionuclide, due to the high cost of the target material used for the main production route ^{64}Ni(p,n)^{64}Cu. To investigate alternative production modalities, the cross sections of the ^{65}Cu(p,pn)^{64}Cu and ^{67}Zn(p, α)^{64}Cu nuclear reactions were measured at the Bern medical cyclotron laboratory, by irradiating enriched ^{65}CuO and enriched ^{67}ZnO targets, respectively. From the results obtained from the cross-section measurements, a study of the production yield and purity was carried out in order to optimize the production of ^{64}Cu.

For the ^{65}Cu(p,pn)^{64}Cu reaction, the produced ^{64}Cu cannot be used to label biomolecules due to the interference of "cold" copper, but can be applied to PET imaging in the [^{64}Cu]$CuCl_2$ form. In this case no other copper radioisotopes are produced in the irradiation but it is necessary to minimize the mass of the irradiated target to avoid possible toxicity issues due to the injection of non-radioactive copper into the patient. According to our findings, by irradiating 30 mg of 99.67% enriched ^{65}Cu with 17.8 MeV protons, a ^{64}Cu production yield of 358 MBq/μA can be achieved at saturation. In this conditions, a clinically relevant dose of 450 MBq corresponds to a copper intake of 0.06 mg Cu/kg for a 60 kg patient, significantly lower than the toxicity limit reported in the literature (>5 mg Cu/kg body weight (Chakravarty et al., 2020; Aggett, 1999)). This value could be further improved by considering a higher beam energy, achievable with research cyclotrons or commercial cyclotrons that can provide at least 26 MeV protons.

By irradiating a 89.60% enriched ^{67}Zn target, the ^{61}Cu and ^{67}Cu impurities are produced by the secondary reactions ^{64}Zn(p, α)^{61}Cu and ^{70}Zn(p, α)^{67}Cu, respectively. Given the low isotopic percentage of ^{70}Zn in the material considered, the ^{67}Cu production in this experiment was negligible. As for ^{61}Cu, whose half-life is much shorter than that of ^{64}Cu, its amount in the sample can be minimized by considering long irradiation times and/or by letting the target decay after EoB. According to our findings, a yield of 479 MBq/μA can be achieved at saturation with a purity of 96%, which increases to 99% within 10 h after the EoB. By considering a ^{67}Zn target with higher enrichment level, copper impurities can be significantly reduced. However, it is necessary to take into account the large amount of gallium radioisotopes produced, which do not affect the purity of ^{64}Cu but make handling the irradiated target and radiochemical processes problematic.

It is important to remark that, if ^{64}Cu is used as a PET diagnostic agent, the presence of ^{61}Cu may not lead to negative effects. It is in fact a β^+-emitter with a shorter half-life, so it does not lead to a higher dose absorbed by the patient and does not produce image degradation effects. Furthermore, the difference in half-life between the two copper radioisotopes could allow the same radiopharmaceutical to be used to follow fast (^{61}Cu based) and slow (^{64}Cu based) metabolic processes. In view of this consideration, it would be interesting to investigate the simultaneous production of ^{64}Cu and ^{61}Cu and possible subsequent clinical applications.

The results reported in this article contribute to the promotion of alternative methods of producing ^{64}Cu using medical cyclotrons in view of theranostic applications in nuclear medicine.

CRediT authorship contribution statement

Gaia Dellepiane: Writing – review & editing, Writing – original draft, Validation, Software, Methodology, Investigation, Formal analysis, Data curation, Conceptualization. **Pierluigi Casolaro:** Writing – review & editing, Investigation. **Isidre Mateu:** Writing – review & editing, Investigation. **Paola Scampoli:** Writing – review & editing, Investigation, Conceptualization. **Saverio Braccini:** Writing – review & editing, Supervision, Resources, Project administration, Methodology, Investigation, Funding acquisition, Conceptualization.

Declaration of competing interest

The authors declare the following financial interests/personal relationships which may be considered as potential competing interests: Saverio Braccini reports financial support was provided by Swiss National Science Foundation.

Data availability

Data will be made available on request.

Acknowledgments

We acknowledge contributions from LHEP engineering and technical staff (Roger Hänni and Jan Christen, in particular) and from the SWAN Isotopen AG team (Riccardo Bosi and Michel Eggemann, in particular). This research project was partially funded by the Swiss National Science Foundation (SNSF) (grants: CRSII5_180352 and 200021_175749).

Appendix

See Tables 6 and 7.

Table 6
Cross-section data of the ^{65}Cu(p,pn)^{64}Cu nuclear reaction.

E [MeV]	^{65}Cu(p,pn)^{64}Cu [mbarn]
12.3 ± 0.4	2.4 ± 0.5
12.7 ± 0.4	4 ± 1
13.1 ± 0.4	9 ± 2
13.8 ± 0.4	26 ± 6
14.5 ± 0.4	54 ± 10
15.2 ± 0.4	82 ± 13
16.0 ± 0.4	129 ± 15
16.4 ± 0.4	142 ± 14
17.1 ± 0.4	177 ± 39
17.5 ± 0.4	191 ± 25
18.2 ± 0.4	222 ± 32

Table 7
Cross-section data of the ^{67}Zn(p, α)^{64}Cu and ^{64}Zn(p, α)^{61}Cu nuclear reactions.

E [MeV]	^{67}Zn(p, α)^{64}Cu [mbarn]	^{64}Zn(p, α)^{61}Cu [mbarn]
5.1 ± 0.5	2.0 ± 0.4	No signal
6.2 ± 0.4	4.0 ± 0.5	3.9 ± 0.9
7.4 ± 0.4	10 ± 2	13 ± 2
8.7 ± 0.4	16 ± 2	31 ± 6
9.7 ± 0.4	23 ± 5	48 ± 9
10.8 ± 0.4	29 ± 5	58 ± 11
12.9 ± 0.4	37 ± 7	85 ± 16
15.0 ± 0.4	37 ± 8	70 ± 13
16.8 ± 0.4	29 ± 4	61 ± 12
18.2 ± 0.4	23 ± 3	43 ± 9

References

Abbas, K., Kozempel, J., Bonardi, M., Groppi, F., Alfarano, A., Holzwarth, U., Simonelli, F., Hofman, H., Horstmann, W., Menapace, E., Lesetický, L., Gibson, N., 2006. Cyclotron production of 64Cu by deuteron irradiation of 64Zn. Appl. Radiat. Isot. 64 (9), 1001–1005. http://dx.doi.org/10.1016/j.apradiso.2005.12.021.

Aggett, P., 1999. An overview of the metabolism of copper. Eur. J. Med. Res. 4, 214–216.

Auger, M., Braccini, S., Carzaniga, T.S., Ereditato, A., Nesteruk, K.P., Scampoli, P., 2016. A detector based on silica fibers for ion beam monitoring in a wide current range. J. Instrum. 11 (03), P03027. http://dx.doi.org/10.1088/1748-0221/11/03/p03027.

Auger, M., Braccini, S., Ereditato, A., Nesteruk, K.P., Scampoli, P., 2015. Low current performance of the Bern medical cyclotron down to the pA range. Meas. Sci. Technol. 26, http://dx.doi.org/10.1088/0957-0233/26/9/094006.

Avila-Rodriguez, M., Rios, C., Carrasco-Hernandez, J., Manrique-Arias, J., Martinez-Hernandez, R., F.O., G.-P., Jalilian, A., Martinez-Rodriguez, E., Romero-Piña, M., Diaz-Ruiz, A., 2017. Biodistribution and radiation dosimetry of [64Cu]copper dichloride: First-in-human study in healthy volunteers. EJNMMI Res. 7 (1), 98–104. http://dx.doi.org/10.1186/s13550-017-0346-4.

Blower, P., Lewis, J., Zweit, J., 1996. Copper radionuclides and radiopharmaceuticals in nuclear medicine. Nucl. Med. Biol. 23 (8), 957–980. http://dx.doi.org/10.1016/s0969-8051(96)00130-8.

Bokhari, T., Mushtaq, A., Khan, I., 2010. Production of low and high specific activity 64Cu in a reactor. J. Radioanal. Nucl. Chem. 284 (2), 265–271. http://dx.doi.org/10.1007/s10967-010-0519-3.

Bonardi, M.L., Groppi, F., Birattari, C., Gini, L., Mainardi, C., Ghioni, A., Menapace, E., Abbas, K., Holzwarth, U., Stroosnijder, M., 2003. Thin-target excitation functions and optimization of simultaneous production of NCA copper-64 and gallium-66,67 by deuteron induced nuclear reactions on a natural zinc target. J. Radioanal. Nucl. Chem. 257, 229–241. http://dx.doi.org/10.1023/A:1024703022762.

Braccini, S., 2013. The new Bern PET cyclotron, its research beam line, and the development of an innovative beam monitor detector. AIP Conf. Proc. 1525, 144–150. http://dx.doi.org/10.1063/1.4802308.

Braccini, S., Aguilar, C.B., Carzaniga, T.S., Dellepiane, G., P. D. Häffner, P.S., 2019. Novel irradiation methods for theranostic radioisotope production with solid targets at the Bern medical cyclotron. Proc. Cyclotrons 2019, http://dx.doi.org/10.18429/JACoW-Cyclotrons2019-TUA02.

Braccini, S., Carzaniga, T.S., Dellepiane, G., Grundler, P.V., Scampoli, P., van der Meulen, N.P., Wüthrich, D., 2022. Optimization of 68Ga production at an 18 MeV medical cyclotron with solid targets by means of cross-section measurement of 66Ga, 67Ga and 68Ga. Appl. Radiat. Isot. 110252. http://dx.doi.org/10.1016/j.apradiso.2022.110252.

Braccini, S., Scampoli, P., 2016. Science with a medical cyclotron. CERN Courier 21–22.

Brinkman, G., Helmer, J., Lindner, L., 1977. Nickel and copper foils as monitors for cyclotron beam intensities. Radiochem. Radioanal. Lett. 28 (1), 9–19.

Capasso, E., Durzu, S., Piras, S., Zandieh, S., Knoll, P., Haug, A., Hacker, M., Meleddu, C., Mirzaei, S., 2015. Role of (64)CuCl2 PET/CT in staging of prostate cancer. Ann. Nucl. Med. 29 (6), 482–488. http://dx.doi.org/10.1007/s12149-015-0968-4.

Capogni, M., Capone, M., Pietropaolo, A., Fazio, A., Dellepiane, G., Falconi, R., Colangeli, A., Palomba, S., Valentini, G., Fantuzi, M., Faccini, R., Pizzuto, A., 2020. 64Cu production by 14 MeV neutron beam. J. Neutron Res. 22 (2–3), 257–264. http://dx.doi.org/10.3233/JNR-190140.

Carzaniga, T.S., Auger, M., Braccini, S., Bunka, M., Ereditato, A., Nesteruk, K.P., Scampoli, P., Türler, A., van der Meulen, N.P., 2017. Measurement of ^{43}Sc and ^{44}Sc production cross-section with an 18 MeV medical PET cyclotron. Appl. Radiat. Isot. 129, 96–102. http://dx.doi.org/10.1016/j.apradiso.2017.08.013.

Carzaniga, T.S., Braccini, S., 2019. Cross-section measurement of ^{44m}Sc, ^{47}Sc, ^{48}Sc and ^{47}Ca for an optimized ^{47}Sc production with an 18 MeV medical PET cyclotron. Appl. Radiat. Isot. 143, 18–23. http://dx.doi.org/10.1016/j.apradiso.2018.10.015.

Casolaro, P., 2021. Radiochromic films for the two-dimensional dose distribution assessment. Appl. Sci. 11 (5), http://dx.doi.org/10.3390/app11052132.

Chakravarty, R., Chakraborty, S., Dash, A., 2016. 64Cu2+ ions as PET probe: An emerging paradigm in molecular imaging of cancer, 13. pp. 3601–3612. http://dx.doi.org/10.1021/acs.molpharmaceut.6b00582.

Chakravarty, R., Shetty, P., Nair, K., Rajeswari, A., Jagadeesan, K., Sarma, H., Rangarajan, V., Krishnatry, R., Chakraborty, S., 2020. Reactor produced [64Cu]CuCl2 as a PET radiopharmaceutical for cancer imaging: From radiochemistry laboratory to nuclear medicine clinic. Ann. Nucl. Med. 34, 899–910. http://dx.doi.org/10.1007/s12149-020-01522-2.

Cohen, B.L., Newman, E., Charpie, R.A., Handley, T.H., 1954. (p, pn) And $(p, \alpha n)$ excitation functions. Phys. Rev. 94, 620–625. http://dx.doi.org/10.1103/PhysRev.94.620.

Collé, R., Kishore, R., Cumming, J., 1976. 65Cu(p,pn)64Cu excitation function in the energy range 13–25 MeV. J. Inorg. Nucl. Chem. 38 (1), 23–25. http://dx.doi.org/10.1016/0022-1902(76)80042-5.

Dellepiane, G., 2022. Activity measurement of a 64Cu sample activated by a 14 MeV neutron beam. IL Nuovo Cimento C 45, http://dx.doi.org/10.1393/ncc/i2022-22084-9.

Dellepiane, G., Aguilar, C.B., Carzaniga, T.S., Casolaro, P., Häffner, P., Scampoli, P., Schmid, M., Braccini, S., 2021. Research on theranostic radioisotope production at the Bern medical cyclotron. IL Nuovo Cimento C 44, http://dx.doi.org/10.1393/ncc/i2021-21130-6.

Dellepiane, G., Casolaro, P., Favaretto, C., Grundler, P.V., Mateu, I., Scampoli, P., Talip, Z., van der Meulen, N.P., Braccini, S., 2022a. Cross section measurement of terbium radioisotopes for an optimized ^{155}Tb production with an 18 MeV medical PET cyclotron. Appl. Radiat. Isot. 184, 110175. http://dx.doi.org/10.1016/j.apradiso.2022.110175.

Dellepiane, G., Casolaro, P., Häffner, P.D., Mateu, I., Scampoli, P., Voeten, N., Zyaee, E., Braccini, S., 2022b. New methods for theranostic radioisotope production with solid targets at the Bern medical cyclotron. EPJ Web Conf. 261, 05006. http://dx.doi.org/10.1051/epjconf/202226105006.

Dellepiane, G., Casolaro, P., Mateu, I., Scampoli, P., Braccini, S., 2023. Appl. Radiat Isot. (In preparation).

Dellepiane, G., Casolaro, P., Mateu, I., Scampoli, P., Voeten, N., Braccini, S., 2022d. Cross-section measurement for an optimized ^{61}Cu production at an 18 MeV medical cyclotron from natural Zn and enriched ^{64}Zn solid targets. Appl. Radiat. Isotopes 190, 110466. http://dx.doi.org/10.1016/j.apradiso.2022.110466.

Favaretto, C., Talip, Z., Borgna, F., Grundler, P.V., Dellepiane, G., Sommerhalder, A., Zhang, H., Schibli, R., Braccini, S., Müller, C., van der Meulen, N.P., 2021. Cyclotron production and radiochemical purification of terbium-155 for SPECT imaging. EJNMMI Radiopharm. Chem. 6, 37. http://dx.doi.org/10.1186/s41181-021-00153-w.

Forgács, A., Balkay, L., Trón, L., Raics, P., 2014. Excel2Genie: A microsoft excel application to improve the flexibility of the Genie-2000 spectroscopic software. Appl. Radiat. Isot. 94, 77–81. http://dx.doi.org/10.1016/j.apradiso.2014.07.005.

Gutfilen, B., Souza, S., G., V., 2018. Copper-64: A real theranostic agent. Drug. Des. Devel. Ther. 2 (12), 3235–3245. http://dx.doi.org/10.2147/DDDT.S170879.

Häffner, P.D., Aguilar, C.B., Braccini, S., Scampoli, P., Thonet, P.A., 2019. Study of the extracted beam energy as a function of operational parameters of a medical cyclotron. Instruments 3 (63), http://dx.doi.org/10.3390/instruments3040063.

Hilgers, K., Stoll, T., Skakun, Y., Coenen, H., Qaim, S., 2003. Cross-section measurements of the nuclear reactions natZn(d,x)64cu, 66Zn(d,alpha)64Cu and 68Zn(p,alphan)64Cu for production of 64Cu and technical developments for small-scale production of 67Cu via the 70Zn(p,alpha)67Cu process. Appl. Radiat. Isot. 59, 343–351. http://dx.doi.org/10.1016/s0969-8043(03)00199-4.

IAEA, 2022. Live chart of nuclides, available online. URL https://nds.iaea.org/relnsd/vcharthtml/VChartHTML.html. (Last Accessed 08 April 2022).

International Standard, 2021. Nuclear Instrumentation – Measurement of Activity Or Emission Rate of Gamma-Ray Emitting Radionuclides – Calibration and Use of Germanium-Based Spectrometers. IEC 61452:2021.

Jauregui-Osoro, M., De Robertis, S., Halsted, P., Gould, S., Yu, Z., Paul, R., Marsden, P., Gee, A., Fenwick, A., Blower, P., 2021. Production of copper-64 using a hospital cyclotron: Targetry, purification and quality analysis. Nucl. Med. Commun. 42 (9), 1024–1038. http://dx.doi.org/10.1097/MNM.0000000000001422.

Kawabata, M., Hashimoto, K., Saeki, H., Sato, N., Motoishi, S., Takakura, K., Konno, C., Nagai, Y., 2015. Production and separation of 64Cu and 67Cu using 14 MeV neutrons. J. Radioanal. Nucl. Chem. 303, 1205–1209. http://dx.doi.org/10.1007/s10967-014-3488-0.

Kin, T., Nagai, Y., Iwamoto, N., Minato, F., Iwamoto, O., Hatsukawa, Y., Segawa, M., Harada, H., Konno, C., Ochiai, K., Takakura, K., 2013. New production routes for medical isotopes 64Cu and 67Cu using accelerator neutrons. J. Phys. Soc. Japan 82, 4201. http://dx.doi.org/10.7566/JPSJ.82.034201.

Koning, A., Rochman, D., 2012. Modern Nuclear Data Evaluation With The TALYS Code System. Nucl. Data Sheets 113, 2841–2934. http://dx.doi.org/10.1016/j.nds.2012.11.002.

Levkowskij, V., 1991. Activation cross sections for the nuclides of Medium Mass Region (A=40-100) with protons and α-particles at medium (E=10-50 MeV) energies. Inter-Vesti, Moscow.

McCarthy, D.W., Shefer, R.E., Klinkowstein, R.E., Bass, L.A., Margeneau, W.H., Cutler, C.S., Anderson, C.J., Welch, M.J., 1997. Efficient production of high specific activity 64Cu using a biomedical cyclotron. Nucl. Med. Biol. 24 (1), 35–43. http://dx.doi.org/10.1016/S0969-8051(96)00157-6.

Meadows, J.W., 1953. Excitation functions for proton-induced reactions with copper. Phys. Rev. 91, 885–889. http://dx.doi.org/10.1103/PhysRev.91.885.

Mirion Technologies, 2022. GENIE 2000 - Basic spectroscopy software. URL https://www.mirion.com/products/genie-2000-basic-spectroscopy-software. (Last Accessed 12 October 2022).

National Center for Biotechnology Information, 2022. PubChem compound summary. URL https://pubchem.ncbi.nlm.nih.gov. (Last Accessed 06 July 2022).

Nesteruk, K.P., Auger, M., Braccini, S., Carzaniga, T.S., Ereditato, A., Scampoli, P., 2018. A system for online beam emittance measurements and proton beam characterization. J. Instrum. 13, P01011. http://dx.doi.org/10.1088/1748-0221/13/01/p01011.

Potkins, D.E., Braccini, S., Nesteruk, K.P., Carzaniga, T.S., Vedda, A., Chiodini, N., Timmermans, J., Melanson, S., Dehnel, M.P., 2017. A low-cost beam profiler based on cerium-doped silica fibers. In: Proceedings of CAARI-16, Physics Procedia. http://dx.doi.org/10.1016/j.phpro.2017.09.061.

Sandia National Laboratories, 2022. InterSpec - Spectral radiation analysis software. URL https://sandialabs.github.io/InterSpec/. (Last Accessed 12 October 2022).

Szelecsényi, F., Blessing, G., Qaim, S., 1993. Excitation functions of proton induced nuclear reactions on enriched 61Ni and 64Ni: Possibility of production of no-carrier-added 61Cu and 64Cu at a small cyclotron. Appl. Radiat. Isot. 44 (3), 575–580. http://dx.doi.org/10.1016/0969-8043(93)90172-7.

Szelecsényi, F., Kovács, Z., Nagatsu, K., Zhang, M.-R., Suzuki, K., 2014. Excitation function of (p,α) nuclear reaction on enriched 67Zn: Possibility of production of 64Cu at low energy cyclotron. Radiochim. Acta 102 (6), 465–472. http://dx.doi.org/10.1515/ract-2013-2145.

Szelecsényi, F., Steyn, G., Kovács, Z., Vermeulen, C., van der Meulen, N., Dolley, S., van der Walt, T., Suzuki, K., Mukai, K., 2005. Investigation of the 66Zn(p,2pn)64Cu and 68Zn(p,x)64Cu nuclear processes up to 100 MeV: Production of 64Cu. Nucl. Instrum. Methods Phys. Res. B 240 (3), 625–637. http://dx.doi.org/10.1016/j.nimb.2005.05.057.

Takacs, S., Tarkanyi, F., Sonck, M., Hermanne, A., 2002. Investigation of the ^{nat}Mo(p,x)$^{96m g}$Tc nuclear reaction to monitor proton beams: New measurements and consequences on the earlier reported data. Nucl. Instrum. Methods Phys. Res. B 198, 183–196.

van der Meulen, N.P., Hasler, R., Talip, Z., Grundler, P.V., Favaretto, C., Umbricht, C.A., Müller, C., Dellepiane, G., Carzaniga, T.S., Braccini, S., 2020. Developments toward the implementation of ^{44}Sc production at a medical cyclotron. Molecules 25, 1–16. http://dx.doi.org/10.3390/molecules25204706.

Ziegler, J.F., Manoyan, J.M., 2013. The stopping of ions in compounds. Nucl. Instrum. Methods B 35, 215, URL http://www.srim.org.

Zinn, K.R., Chaudhuri, T.R., Cheng, T.-P., Steven Morris, J., Meyer Jr., W.A., 1994. Production of no-carrier-added 64Cu from zinc metal irradiated under boron shielding. Cancer 73 (S3), 774–778. http://dx.doi.org/10.1002/1097-0142(19940201)73:3+<774::AID-CNCR2820731305>3.0.CO;2-L.